BRAIN
A JOURNAL OF NEUROLOGY

Epileptic high-frequency network activity in a model of non-lesional temporal lobe epilepsy

Premysl Jiruska,[1] Gerald T. Finnerty,[2,3] Andrew D. Powell,[1] Noosheen Lofti,[1] Roman Cmejla[4] and John G. R. Jefferys[1,3]

1 Neuronal Networks Group, School of Clinical and Experimental Medicine, University of Birmingham, Birmingham B15 2TT, UK
2 MRC Centre for Neurodegeneration Research, King's College London, Institute of Psychiatry, London SE5 8AF, UK
3 Department of Physiology and Biophysics, Imperial College of Science Technology and Medicine (St Mary's), London W2 1PG, UK
4 Department of Circuit Theory, Faculty of Electrical Engineering, Czech Technical University, Prague 16635, Czech Republic

Correspondence to: John G. R. Jefferys,
Neuronal Networks Group, School of Clinical and Experimental Medicine,
College of Medical and Dental Sciences, University of Birmingham,
Birmingham B15 2TT, UK
E-mail: j.g.r.jefferys@bham.ac.uk

High-frequency cortical activity, particularly in the 250–600 Hz (fast ripple) band, has been implicated in playing a crucial role in epileptogenesis and seizure generation. Fast ripples are highly specific for the seizure initiation zone. However, evidence for the association of fast ripples with epileptic foci depends on animal models and human cases with substantial lesions in the form of hippocampal sclerosis, which suggests that neuronal loss may be required for fast ripples. In the present work, we tested whether cell loss is a necessary prerequisite for the generation of fast ripples, using a non-lesional model of temporal lobe epilepsy that lacks hippocampal sclerosis. The model is induced by unilateral intrahippocampal injection of tetanus toxin. Recordings from the hippocampi of freely-moving epileptic rats revealed high-frequency activity (>100 Hz), including fast ripples. High-frequency activity was present both during interictal discharges and seizure onset. Interictal fast ripples proved a significantly more reliable marker of the primary epileptogenic zone than the presence of either interictal discharges or ripples (100–250 Hz). These results suggest that fast ripple activity should be considered for its potential value in the pre-surgical workup of non-lesional temporal lobe epilepsy.

Introduction

High-frequency (>100 Hz) cortical activity (HFA) has been linked to epileptic activity in humans and in experimental models (Allen *et al.*, 1992; Fisher *et al.*, 1992; Bragin *et al.*, 1999a; Worrell *et al.*, 2004; Jacobs *et al.*, 2008). Recent experimental evidence suggests it is associated with the development of epileptic foci (epileptogenesis) (Bragin *et al.*, 2004) and in seizure initiation

(ictogenesis) (Bragin *et al.*, 2005). *In vivo* activity from frequency band 200–500 Hz has proved highly specific for epileptic foci (Bragin *et al.*, 1999a). The majority of studies describing experimental epileptic HFA used the kainate or pilocarpine models of temporal lobe epilepsy, which depend on the establishment of a substantial hippocampal lesion akin to hippocampal sclerosis (Bragin *et al.*, 2004; Foffani *et al.*, 2007). In this and other models that depend on an initial period of status epilepticus,

the morphological and functional alterations associated with the substantial neuronal loss have been implicated in the establishment of the chronic epileptic focus. Recently, the loss of neurons in the pilocarpine model has been implicated in the generation of epileptic high-frequency activity, and specifically for the shift from ripple frequencies (100–300 Hz) to fast ripple frequencies (200–600 Hz) (Foffani et al., 2007). In the present study, we use the intrahippocampal tetanus toxin model of non-lesional temporal lobe epilepsy (Hawkins and Mellanby, 1987; Jefferys et al., 1992; Jefferys and Walker, 2005) to test the hypothesis that neuronal loss is a prerequisite for the fast ripples of epileptic HFA.

Materials and methods

Surgery and electrode implantation

Male Sprague-Dawley rats (280–400 g) were anaesthetized with halothane. Bipolar recording electrodes (twisted Teflon-coated 125 μm diameter stainless steel wire; Medwire Corp, New York; with the tips separated 250–350 μm along the axis of the wires) were placed into CA3 and either CA1 or dentate granule cell body layers of both cerebral hemispheres, with the second pole in stratum radiatum (CA1, CA3) or stratum moleculare (dentate gyrus), using the evoked response produced by ventral commissural stimulation as a guide (Finnerty and Jefferys, 1993). Coordinates were: CA3, 2.7 mm posterior and 3.3 mm lateral to bregma and initially 3.9 mm below cortical surface; CA1, 3.1 mm posterior, 2.9 mm lateral and initially 2.1 mm deep; and dentate gyrus, 3.1 mm posterior, 3.3 mm lateral and initially 3.3 mm deep. One microlitre of phosphate buffered saline plus bovine serum albumin, either without (three controls) or with 4–5 ng (12 mouse LD_{50}; 10 rats) tetanus toxin (kind gift of the Wellcome Foundation, Beckenham, UK) was injected into the right hippocampus, 2.7 mm posterior, 3.5 mm lateral and 3.5 mm below the cortical surface. An antibiotic (Panalog, Fort Dodge) was applied to the wound edge to avoid infection under the skin or headstage and the animals were allowed to recover under supervision in separate cages. After recovery from anaesthesia, the animals were housed separately postoperatively with free access to food and water, allowed 24–48 h to recover, and then handled gently to familiarize them with the recording procedure. All toxin-injected rats developed spontaneous seizures 4 or more (typically 7–10) days after surgery and none died. None of the control-injected rats developed seizures.

Recordings in vivo

Recording started 3–6 days postoperatively. The headstage contacts were connected, via counterbalanced wires, to a slip ring and preamplifier and then to differential amplifiers (Digitimer D160, band-pass: 0.5 Hz to 3 kHz, and DC to 3 kHz for six seizures). The amplified EEG signal was stored on FM tape (Racal V Store, Racal, Southampton, UK bandpass DC-3.25 kHz). Selected recordings from animals with fully developed epilepsy were made between 3 and 21 days after injection, and digitized using a signal acquisition system (1401, Cambridge Electronic Design, Cambridge, UK) at a sampling frequency of 2.5 kHz. After completion of the recording protocol, the animal was euthanized with an overdose of halothane. The brain was dissected out, fixed in formalin, and embedded in wax, prior to staining 10 μm parasagittal sections with cresyl fast violet or haematoxylin and eosin to confirm the electrode sites and examine for any morphological abnormalities.

Data analysis

Signal epochs lasting 0.3 s (ictal onset) or 0.5 s (interictal events) were analysed using Morlet wavelet transforms to determine their spectral composition (Li et al., 2007). Power spectra were calculated both from raw data and from data filtered by a high-pass filter (>100 Hz Finite Impulse Response filter). To quantify power spectra of signals and compare differences in spectral composition, we used an unbiased method by calculating the median, first spectral moment and second spectral moment of the acquired power spectra. Spectral moments were used to characterize the power of a signal over its bandwidth. The first spectral moment (or mean frequency, or spectral centre of gravity) is a weighted average and is a useful measure of the concentration of the signal power over its frequency range. First moment mom_1 was calculated using following formula, where f is frequency and I is power.

$$mom_1 = \frac{\sum f.I}{\sum I}$$

The second spectral moment mom_2 (analogous to the statistical variance) gives an indication of how spread-out or diffuse the spectrum is. All measures were calculated for the frequency band 100–1000 Hz.

$$mom_2 = \sqrt{\frac{\sum f^2.I}{\sum I} - \left(\frac{\sum f.I}{\sum I}\right)^2}$$

The ratio between the summated powers in the fast ripple (251–600 Hz) and ripple (100–250 Hz) bands was used to characterize electrophysiological data. Spectrograms with high temporal resolution were created calculating power spectra from 50 to 100 ms windows, with 90% overlap of adjacent windows, and presented as pseudo-colour plots.

To quantify the numbers of fast ripple and ripple events we implemented an automated, unbiased method to detect HFA events similar to that developed by Staba et al. (2002). Artefact-free epochs of interictal recording 1000 s in duration were selected and band-pass (100–600 Hz) filtered using a Finite Impulse Response filter. The standard deviation of the signal was calculated across the entire epoch. A sliding window of 200 ms was moved along the signal in steps of 200 ms. Windows with signal standard deviations greater than twice the whole epoch standard deviation were selected for further analysis. Within each of these selected windows individual spikes with amplitudes greater than five times the epoch standard deviation were identified. If more than six cycles were detected in the epoch then the median interspike interval was measured. If the median interspike interval was less than 4 ms then the event was identified as a fast ripple; if the median interspike interval was between 4 and 10 ms the event was identified as a ripple. The incidence of ripples or fast ripple events was expressed as rate per 10 min following the convention of Staba et al. (2002).

To examine synchronization between areas, intrahippocampal and interhippocampal coherence was calculated. For each animal, the coherence was derived from 40 epochs of 1 s duration, each containing episodes of HFA superimposed on interictal discharges. Coherence was calculated using Welch's averaged modified periodogram with a window size of 128 samples (19.5 ms) and 50% overlap between successive windows. To assess the reliability of the coherence estimate, 95% confidence intervals were calculated using jack-knife statistics Chronux package (http://www.chronux.org) (Mitra and Pesaran, 1999).

Coherence is a function of the power spectral density (P_{xx} and P_{yy}) of signals x and y and their cross power spectral density (P_{xy}). Coherence estimates the strength of any linear relationship between two signals at each frequency. Its values range from 0 to 1.

$$Cxy(f) = \frac{|Pxy(f)|^2}{Pxx(f)Pyy(f)}$$

Statistical analyses included t-test, Mann–Whitney test, Kolmogorov–Smirnov test and Fisher's exact test, and were used as indicated in the text. All results are expressed as mean $\pm$ SEM.

Results

Interictal activity and high-frequency cortical activity

In the present study we recorded hippocampal activity from rats with fully developed epilepsy and spontaneous seizures. Electrodes were located in CA3 on both sides in all 10 animals, and a second set of electrodes was placed in each hippocampus in either CA1 (seven animals) or dentate gyrus (three animals). The interictal periods (between seizures) were characterized by brief synchronous interictal discharges. These discharges were transient spikes or sharp waves of variable duration and polarity. Differences in polarity are due to the precise locations of the bipolar electrodes in the hippocampal laminae. Interictal activity was recorded from the right, injected (henceforth ipsilateral) hippocampus alone (Fig. 1A) or from both hippocampi synchronously (Fig. 1B and D) in all 10 animals. In 4 of the 10 animals, interictal discharges were recorded from the contralateral hippocampus alone (Fig. 1C), and were more frequent than discharges originating from the ipsilateral hippocampus. The leading interictal discharge was most commonly recorded in the CA3 area of the ipsilateral hippocampus. Previous

observations *in vitro* also showed that interictal discharges were initiated in CA3 (Jefferys, 1989).

Interictal discharges were associated with HFA, which was superimposed on the interictal discharges (Fig. 2). HFA was observed on $71 \pm 7\%$ of interictal discharges in the ipsilateral hippocampus in all 10 animals, whereas in contralateral hippocampus it was observed in five of 10 animals where they represented $48 \pm 11\%$ of interictal discharges (incidence not significantly different from ipsilateral hippocampus, Fig. 3B). The remaining five animals produced contralateral interictal discharges without HFA. If observed contralaterally, HFA usually occurred during bilaterally synchronous discharges (Fig. 1B and D), but in three animals HFA could also be observed during independent contralateral discharges. Although HFA could be observed in either hippocampus, its presence was significantly more common in the ipsilateral hippocampus (Fisher's exact test; $P<0.05$). HFA could be observed in all hippocampal subregions: CA3, CA1 and dentate gyrus on both sides. Its morphology, amplitude and frequency varied (Fig. 2). The HFA waveform varied from spike-like (triangular) cycles (Fig. 4F) to a sinusoidal oscillatory pattern (Fig. 4E). Amplitudes ranged from $30\,\mu V$ up to $1.9\,mV$. The mean amplitude of HFA was higher in contralateral hippocampus then in ipsilateral ($P<0.001$, Table 1). The frequency of HFA spanned the ripple and fast ripple bands (100–600 Hz; the demarcation between the bands is between 200 and 300 Hz, depending on the study). During individual interictal discharges, HFA frequency could shift from fast ripple frequencies to ripple frequencies or vice versa (Fig. 4). HFA could occur at any stage in the course of the interictal discharges (Fig. 2), but its highest probability of occurrence was during the peak of the discharges (Fig. 3A).

Median, first and second moments of the power spectrum for each episode of HFA were calculated to characterize its frequency profile (Table 1). The location of the peaks varied between rats, but was relatively consistent for each region in individual rats.
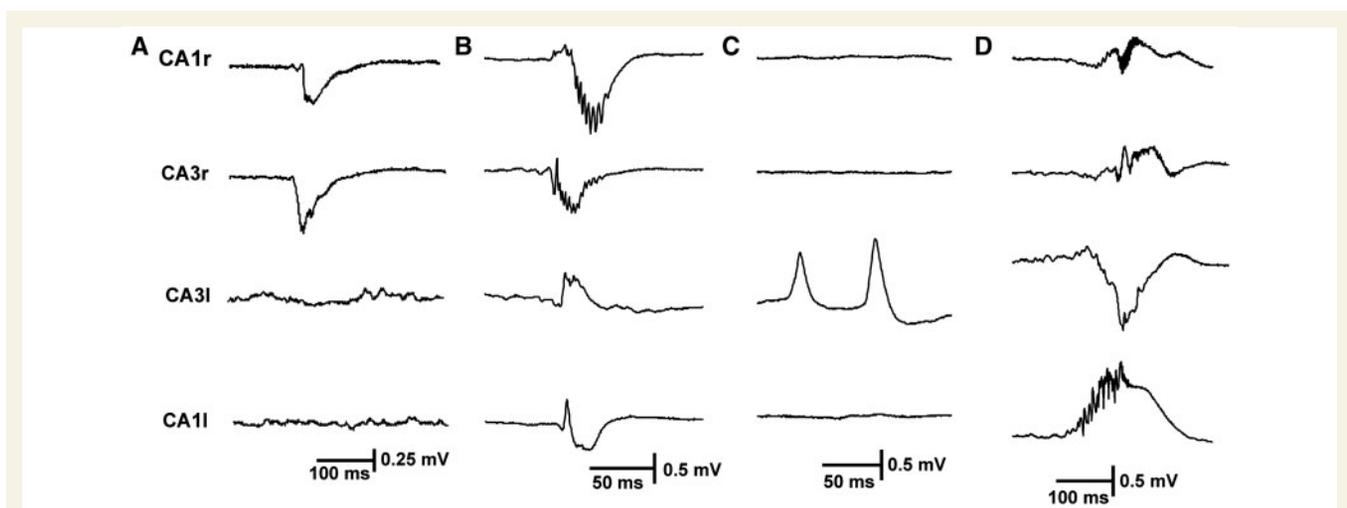
Figure 1 Interictal discharges in the intrahippocampal tetanus toxin model of epilepsy. (**A**) Unilateral discharges originating in ipsilateral CA3, spreading to ipsilateral CA1. (**B**) Bilateral synchronous discharge, originating in ipsilateral CA3. In the ipsilateral hippocampus HFA is superimposed on interictal discharges. (**C**) Contralateral independent CA3 interictal discharges. (**D**) Bilateral synchronous discharges originating in contralateral CA1 with propagation to ipsilateral hippocampus. HFA is an integral part of the ipsi- and contralateral CA1 discharges. All panels are of raw data (0.5 Hz to 1 kHz).
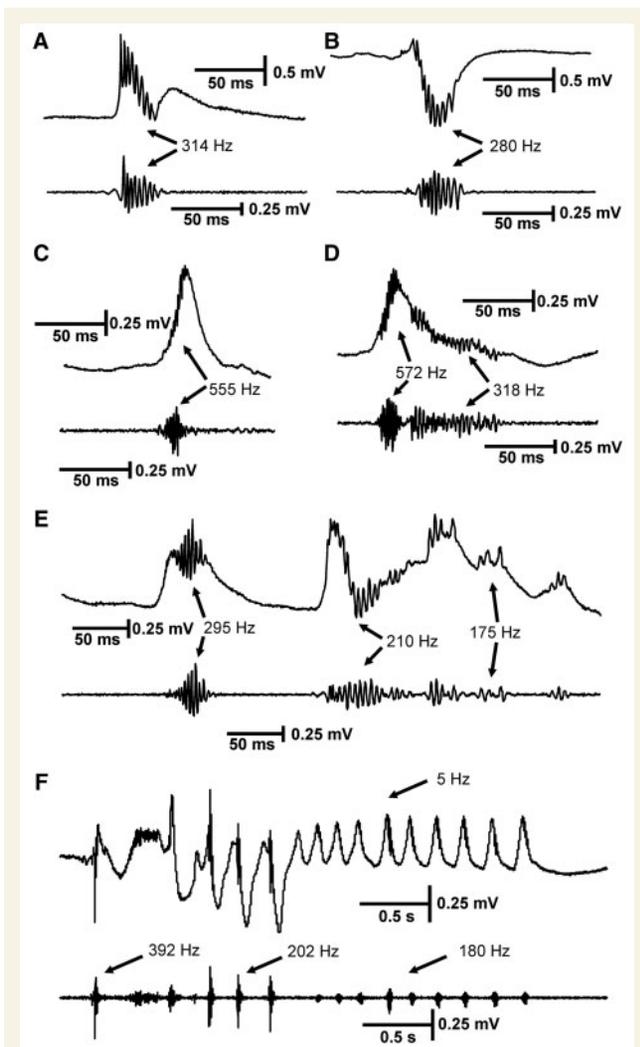
The spectrum in Fig. 3D is based on a single epoch of 0.5 s including an interictal discharge as shown in Fig. 3C. The first spectral moment in this case was 359 Hz (Fig. 3D; averaged spectra for all rats are shown in Supplementary Fig. 1). The mean, across all the epileptic rats, of the first spectral moments in the ipsilateral hippocampus was 331 ± 4 Hz. During bilaterally synchronous interictal discharges, the first spectral moment in the contralateral hippocampus was 235 ± 6 Hz (Fig. 3E). During independent contralateral discharges the first spectral moment was 243 ± 4 Hz. HFA occurred preferentially in the ipsilateral hippocampus, where it had significantly higher frequencies than in contralateral hippocampus (Fig. 3E), whether during bilaterally

Figure 2 Different types of high-frequency activity in the tetanus toxin model of temporal lobe epilepsy. High-frequency activity is superimposed on interictal discharges, most often during their peaks, but in some cases earlier or later. HFA of different frequencies can be observed (**A–F**), in some cases during individual interictal discharges (**D**, **E**). The marked frequency values are the peak frequency of the power spectra. (**F**) Repeated epileptiform discharges with frequency ~5 Hz: HFA is present throughout its course, but varies in amplitude and frequency. In each panel the top trace consists of raw data and the bottom is band-pass filtered 100–600 Hz.

synchronous or independent interictal discharges. The between-sides differences were also present within each of the hippocampal subregions recorded here (Fig. 3F). Most often the epileptic HFA was most pronounced in CA1 ipsilateral to the injection, where it has its maximum amplitude but the highest frequency was observed in CA3 ipsilateral to the injection (Fig. 3F). The ratio of summated powers in the fast ripple and ripple bands also was significantly higher in the ipsilateral hippocampus than in the contralateral (Fig. 3G), and in the contralateral hippocampus was significantly higher in bilaterally synchronous than independent interictal discharges (1.03 ± 0.12 and 0.54 ± 0.04, respectively). The inter-hemisphere difference in fast ripple/ripple ratio was consistent in each of the hippocampal subregions (Fig. 3H).
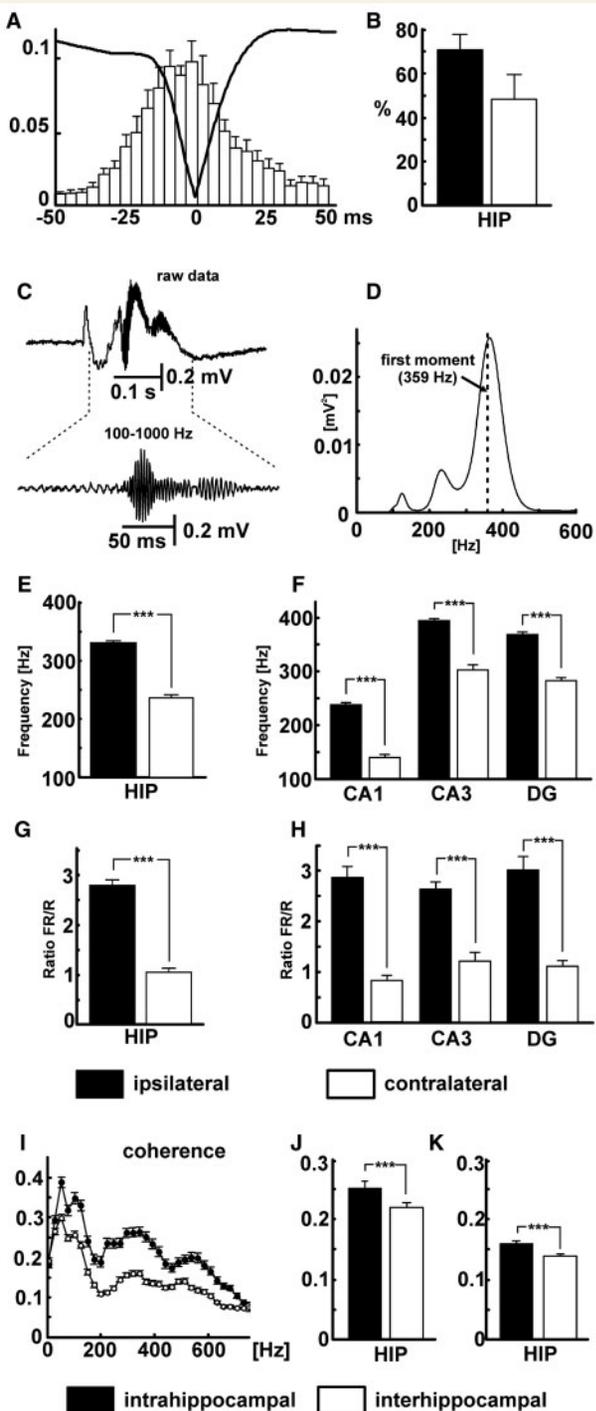
To understand which features of the HFA signals contribute to the high-frequency peaks in the power spectra, we calculated instantaneous frequencies from (i) inter-cycle intervals between adjacent cycles of HFA (Fig. 4C); and (ii) the width of individual cycles measured to the inflections either side of the negative spike (Fig. 4D). Both measures are less sensitive to the shape of the cycle waveform than the spectral analysis of the complete signal. Both inter-cycle interval and cycle width confirmed the presence of oscillations in the fast ripple and ripple bands (Fig. 4C and D). If the original signal had a sinusoidal (oscillatory) pattern (Fig. 4E) then it usually manifested with single peak in the power spectrum, visible in Fig. 4G as the substantial fast ripple band centred on 564 Hz between 30 and 60 ms. This pattern shows that fast ripples are not necessarily harmonics of simultaneous ripple band activity, as they are between 90 and 110 ms during the interictal discharge in Fig. 4G, and in Foffani *et al.* (2007). Where HFA contains harmonics (e.g. at 275 and 540 Hz in Fig. 4G), the individual cycles have a complex waveform (Fig. 4F) that was often triangular (spike-like) or appeared to have very small interposed cycles that could indicate out-of-phase firing.

In order to determine the rate of ripples and of fast ripples that were not harmonics due to a non-sinusoidal ripple waveform, we used an unbiased method to identify HFA events of six or more cycles based on thresholding HFA cycles at five times the overall signal standard deviation and characterized them as ripples and fast ripples by their median interspike intervals (Fig. 5A and B). Using this method we found that the rate of ripple events did not differ between ipsilateral (24.7 ± 7.4 per 10 min) and contralateral (15.1 ± 7.3 per 10 min; Fig. 5C). However the rate of fast ripple events in the ipsilateral hippocampus (19.0 ± 9.2 per 10 min) was significantly greater than in the contralateral (3.4 ± 2.6 per 10 min; Mann–Whitney test; $P < 0.05$; Fig. 5D). In all 10 rats the rate of fast ripples was greater in the ipsilateral hippocampus than the contralateral, and in 5 out of 10 rats the contralateral hippocampal recordings revealed no fast ripples at all (Fig. 5E).

Coherence analysis assessed the synchrony of HFA between hippocampal subregions (intrahippocampal coherence) and between hippocampi (interhippocampal coherence) during periods when pairs of signals both contained HFA (Fig. 3I). Intrahippocampal coherence was stronger than interhippocampal in both the ripple band (0.25 ± 0.01 and 0.16 ± 0.01; Fig. 3J) and fast ripple band (0.22 ± 0.01 and 0.14 ± 0.01; Fig. 3K; Mann–Whitney tests $P < 0.001$ in both cases). The higher coherence values for

Figure 3 Properties of HFA. (**A**) Averaged interictal discharge waveform superimposed on cross-correlation between HFA and interictal discharge shows that HFA can be observed throughout the entire course of interictal discharge with maximal probability of occurrence during the peak of interictal discharge. (**B**) Proportion of interictal discharges with superimposed HFA in ipsilateral (filled bar) and contralateral (open bar) hippocampi. (**C**) Epoch lasting 0.5 s including an interictal discharge, with expansion of band-pass filtered HFA below, recorded from ipsilateral CA3. (**D**) Corresponding power spectrum for the band passed 0.5 s interictal epoch shown in **C** (dashed line shows first moment at 359 Hz). (**E**) Comparison of first spectral moment in ipsilateral and contralateral hippocampi. (**F**) First spectral moments in subregions of ipsilateral and contralateral hippocampi. (**G**) Comparison of ratio of fast ripple (FR) to ripple (R) power in ipsi- and contralateral hippocampi (i.e. the summated HFA powers below and above 250 Hz for all interictal events in all epileptic rats). (**H**) Ratios of fast ripple to ripple power in subregions of ipsilateral and contralateral hippocampi. (**I**) Intrahippocampal (filled symbols) and interhippocampal (open symbols) coherence. (**J**) Mean values of intra- and inter-hippocampal coherence for ripple band (filled and open bars, respectively). (**K**) Mean values of coherence for fast ripple band. (Error bars represent SEM, significance values are ***$P < 0.001$). DG = dentate gyrus; HIP = hippocampi.

very low frequencies probably represent propagation of, and synchrony between, the low-frequency components of interictal discharges.

In 9 out of 10 animals we observed repeated epileptiform discharges of various frequencies between 3 and 7 Hz, essentially short bursts of discharges that resembled the initial parts of seizures (Fig. 2F). These repeated epileptiform discharges occurred as local phenomena either in the ipsilateral hippocampus alone (three animals) or synchronously in both hippocampi (six animals), and never in the contralateral hippocampus alone. HFA was superimposed on repeated epileptiform discharges during their initial parts and/or throughout their full course. If the repeated epileptiform discharge propagated to the contralateral hippocampus, HFA occurred preferentially in the ipsilateral hippocampus.

None of the interictal epileptiform phenomena described above was observed in the three control animals injected with vehicle.
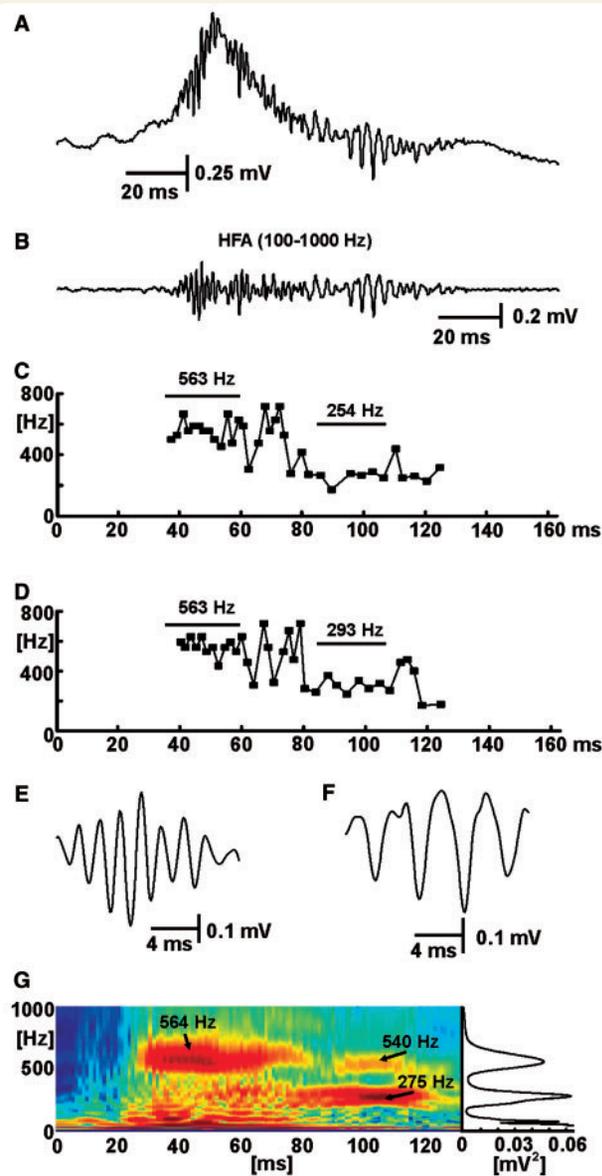
Ictal activity and high-frequency cortical activity

All animals in this study developed epilepsy characterized by spontaneous recurrent seizures, which were classified as complex partial seizures with secondary generalization. The 60 electrographic seizures recorded were characterized by two distinct onset patterns. The most common was hypersynchronous onset ('HYP' in Engel, 1990), which occurred in 83% of seizures and was characterized by initial high-amplitude slow waves on which HFA could be superimposed (Fig. 6A and B). These hypersynchronous-onset seizures had focal onsets followed by rapid propagation (within ∼5 ms) to other ipsi- and contralateral areas (Finnerty and Jefferys, 2002). The second seizure pattern was characterized by a progressive build-up of ictal discharges (low-amplitude fast activity onset, or 'LVF'; Engel, 1990; Bragin *et al.*, 2005). This seizure pattern had a clear local onset with slower propagation, and occurred in 14% of recorded seizures.

The majority of seizures (73%) started in ipsilateral hippocampus with 63% originating in ipsilateral CA3 and 10% in ipsilateral CA1. Seizures with contralateral onset were observed in 27% of seizures and all of them originated from contralateral CA3.

HFA occurred throughout the seizures (Fig. 6C) but here we focus on HFA at seizure onset (Fig. 6B). This ictal-onset HFA was present at the onset of 'synchronous' types of seizures. In contrast to interictal HFA, the presence of ictal-onset HFA did not differ statistically between ipsilateral and contralateral

Figure 4 Interspike interval and cycle width and waveform shape contribute to spectral profile of epileptic HFA. (**A**) Interictal discharge with superimposed HFA of varying frequencies. (**B**) Band-passed filtered data (100–1000 Hz) from **A** showing isolated HFA. (**C**) Instantaneous frequency plot derived from the interspike interval between minima of successive HFA cycles from **B**. (**D**) Instantaneous frequency derived from the width of individual spikes from **B**, measured between maxima either side of the spikes. (**E**) Waveform of fast HFA. Note the sinusoidal shape of the waveform. (**F**) Waveform of HFA at a lower frequency, which has a more pronounced triangular (spike-like) shape: individual spikes start and stop at local maxima that result in the shorter periods (and faster instantaneous frequency) in the later segment of panel **D**. (**G**) Wavelet spectrogram corresponding to data in panel **A**, with the corresponding power spectrum projected to the right to illustrate how the dynamic changes revealed in the spectrogram are represented in conventional power spectra. In **G** the full false colour scale spans −10 to −2 log(mV²).

hippocampi (10/10 and 7/10, respectively; Fisher's exact test, $P > 0.05$). High-frequency activity at the onset of seizures had similar morphology to that during interictal activity. Amplitudes of HFA did not significantly differ between ipsilateral and contralateral hippocampus (Table 1). HFA amplitudes at seizure onset reached up to 1.2 mV. Ictal-onset HFA showed significant differences in frequency, with higher frequencies in the ipsilateral hippocampus than the contralateral (first spectral moments respectively 339 ± 76 and 220 ± 9 Hz; Table 1). We separated the contralateral onset seizures from pooled data and found that the ipsilateral hippocampi still had faster HFA than the contralateral (first spectral moments 403 ± 16 and 261 ± 10 Hz, respectively), therefore the ipsilateral hippocampus generates the faster HFA irrespective of side of seizure onset. HFA from ipsilateral and contralateral hippocampus also could be differentiated by the fast ripple:ripple ratio, which was significantly higher in the ipsilateral hippocampus than the contralateral. Spectra also differed between regions (Fig. 6E and G): median frequency was significantly higher in ipsilateral CA3 than contralateral (261 ± 8 and 217 ± 16 Hz, respectively; t-test, $P < 0.001$). Ipsilateral and contralateral CA1 areas significantly differed in medians of power spectra (t-test, $P < 0.01$) and fast ripple/ripple ratio (t-test; $P < 0.05$), but not in the first spectral moments.

Histology

The animals in this study were routinely examined post-mortem to confirm the location of the injection, determined by a track of local damage a few tens of microns wide, and to detect any neuropathology (Fig. 7). We have previously shown that this model produces no neuronal loss in the hippocampus in >90% of rats, and that the remaining <10% have a focal lesion in CA1 with a near-complete loss of pyramidal cells within a ~1 mm diameter region and normal neuronal density outside that region (Jefferys *et al.*, 1992). Similar sporadic focal lesions of dorsal CA1 have been reported following ventral injections of low-dose tetanus toxin (Shaw *et al.*, 1990; Mitchell *et al.*, 1995, 1996). In the present study histological sections were obtained from 7 of the 10 animals. All of the animals processed in this manner revealed that the injection was located within the hippocampal CA3 region, and the electrodes were located in or near the cell body layers of CA3 and CA1 or dentate gyrus. None of the sections revealed neuronal loss apart from the local damage around the needle track, which was similar in toxin- and control-injected cases. The epilepsy-related lesions characteristic of a minority of rats in this model (Shaw *et al.*, 1990; Jefferys *et al.*, 1992; Mitchell *et al.*, 1995, 1996) would have been immediately obvious on these sections. Figure 7 shows an example with documented fast ripples in the ipsilateral hippocampus; contralateral hippocampus also lacked neuronal loss (Supplementary Fig. 2 shows contralateral hippocampus).

Discussion

The central conclusion of this study is that epileptic high-frequency activity, consisting of both ripples and fast ripples, occurs in a

Table 1 Measurements of interictal and ictal epileptic discharges from ipsilateral and contralateral hippocampi of the 10 epileptic rats

Interictal	Ipsilateral HFA (n = 760)	Contralateral HFA (n = 320)	Significance (t-test)
Interictal discharge amplitude	0.76 ± 0.02 mV	1.13 ± 0.04 mV	$P < 0.001$
Interictal discharge duration	78 ± 1 ms	90 ± 3 ms	$P < 0.001$
Amplitude	0.25 ± 0.01 mV	0.34 ± 0.02 mV	$P < 0.001$
First spectral moment	331 ± 4 Hz	235 ± 6 Hz	$P < 0.001$
Second spectral moment	180 ± 2 Hz	153 ± 3 Hz	$P < 0.001$
Median	295 ± 4 Hz	191 ± 6 Hz	$P < 0.001$
Fast ripple/ripple ratio	2.77 ± 0.11	1.03 ± 0.12	$P < 0.001$
Ictal	(n = 92)	(n = 65)	Significance (t-test)
Amplitude	0.24 ± 0.02 mV	0.21 ± 0.02 mV	NS
First spectral moment	339 ± 8 Hz	281 ± 8 Hz	$P < 0.001$
Second spectral moment	188 ± 6 Hz	185 ± 4 Hz	NS
Median	293 ± 9 Hz	220.2 ± 9.1 Hz	$P < 0.001$
Fast ripple/ripple ratio	1.76 ± 0.16	0.87 ± 0.11	$P < 0.001$
Seizure onset	73%	27%	

Interictal discharge amplitude and duration (first two rows) are the means and SEM of these epileptic events recorded wide-band. The bottom row indicates the percentages of seizures starting in the ipsilateral (injected) and contralateral hippocampi. All the remaining measurements are of the high frequency activity (100–600 Hz) superimposed on epileptic discharges, both interictal and ictal. Statistical tests are comparisons of ipsilateral and contralateral data. NS = not significant.
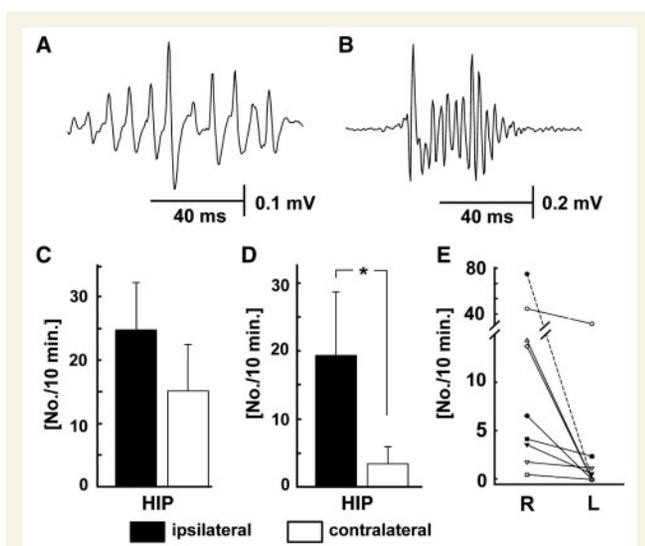

Figure 5 Ripples and fast ripples detected by spike thresholding. (**A**) Typical ripple event from contralateral hippocampus. (**B**) Typical fast ripple event from ipsilateral hippocampus. (**C**) The incidence of ripples per 10 min did not differ between hippocampi. (**D**) The incidence of fast ripples per 10 min was significantly greater in the ipsilateral hippocampus [$P < 0.05$, Mann–Whitney test, (*)]. (**E**) in all cases the incidence of fast ripples was greater in the ipsilateral hippocampus (R), and in 5 of 10 animals was zero in the contralateral (L).

non-lesional model of temporal lobe epilepsy induced by unilateral intrahippocampal injection of tetanus toxin. Our data show that HFA is present during both interictal discharges and seizure onset. Fast ripples occur in all subregions studied: dentate gyrus, CA3 and CA1; previous reports on chronic foci *in vivo* have not reported fast ripples in CA3 (Bragin *et al.*, 1999a, 2005), a difference that could be due to electrode positioning or to the preservation of CA3 in the present tetanus toxin model. Both

hippocampi are capable of generating high-frequency activity, but it occurs preferentially in the ipsilateral hippocampi, where the frequency of HFA is in the fast ripple band. Bragin *et al.* (1999a) argue that fast ripples are a marker for brain areas capable of initiating spontaneous seizures both in the rat kainate model and in human temporal lobe foci (Bragin *et al.*, 1999a; Staba *et al.*, 2002). The association between fast ripples and the injected hippocampus in the tetanus toxin model supports this idea. The present report shows that substantial neuronal loss and hippocampal sclerosis, characteristic of previous reports (Bragin *et al.*, 1999b; Foffani *et al.*, 2007; Staba *et al.*, 2007), are not prerequisites for fast ripple activity associated with epileptic foci.

The mechanisms for fast ripples are still a matter of active debate. Physiological ripples (<250 Hz) have been attributed to local interneuronal activity generating fast synchronous inhibitory postsynaptic potentials on pyramidal cells (Ylinen *et al.*, 1995). They are normally driven by synchronous CA3 input into CA1 producing sharp-wave ripples, where the ripples occur at ~180 Hz. At the cellular level this mechanism leads to coordinated firing of pyramidal cells, which is thought to be important in the process of memory formation and memory consolidation (Axmacher *et al.*, 2006). This mechanism does not appear fast enough to generate fast ripples.
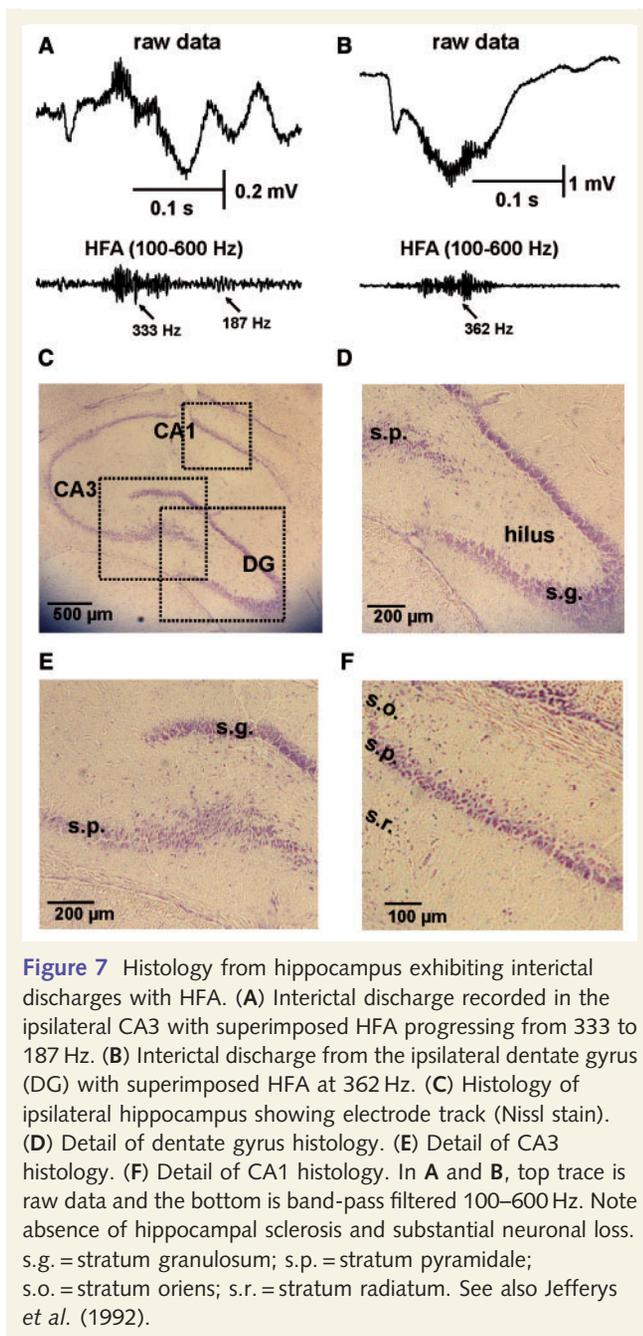
In many situations individual HFA cycles can be shown to represent small population spikes due to synchronous firing of small groups of principal cells (pyramidal cells or granule cells) (Draguhn *et al.*, 1998; Bragin *et al.*, 1999a, 2000; Bikson *et al.*, 2003; Jiruska *et al.*, 2010). Several mechanisms have been proposed to synchronize principal cell firing on the timescale of a few milliseconds required for ripples and fast ripples: excitatory synaptic coupling (Dzhala and Staley, 2004), gap junction coupling (Draguhn *et al.*, 1998) and ephaptic or field effect interactions (Snow and Dudek, 1984; Dudek *et al.* 1986; Jefferys, 1995; Bikson *et al.*, 2003; Grenier *et al.*, 2003).
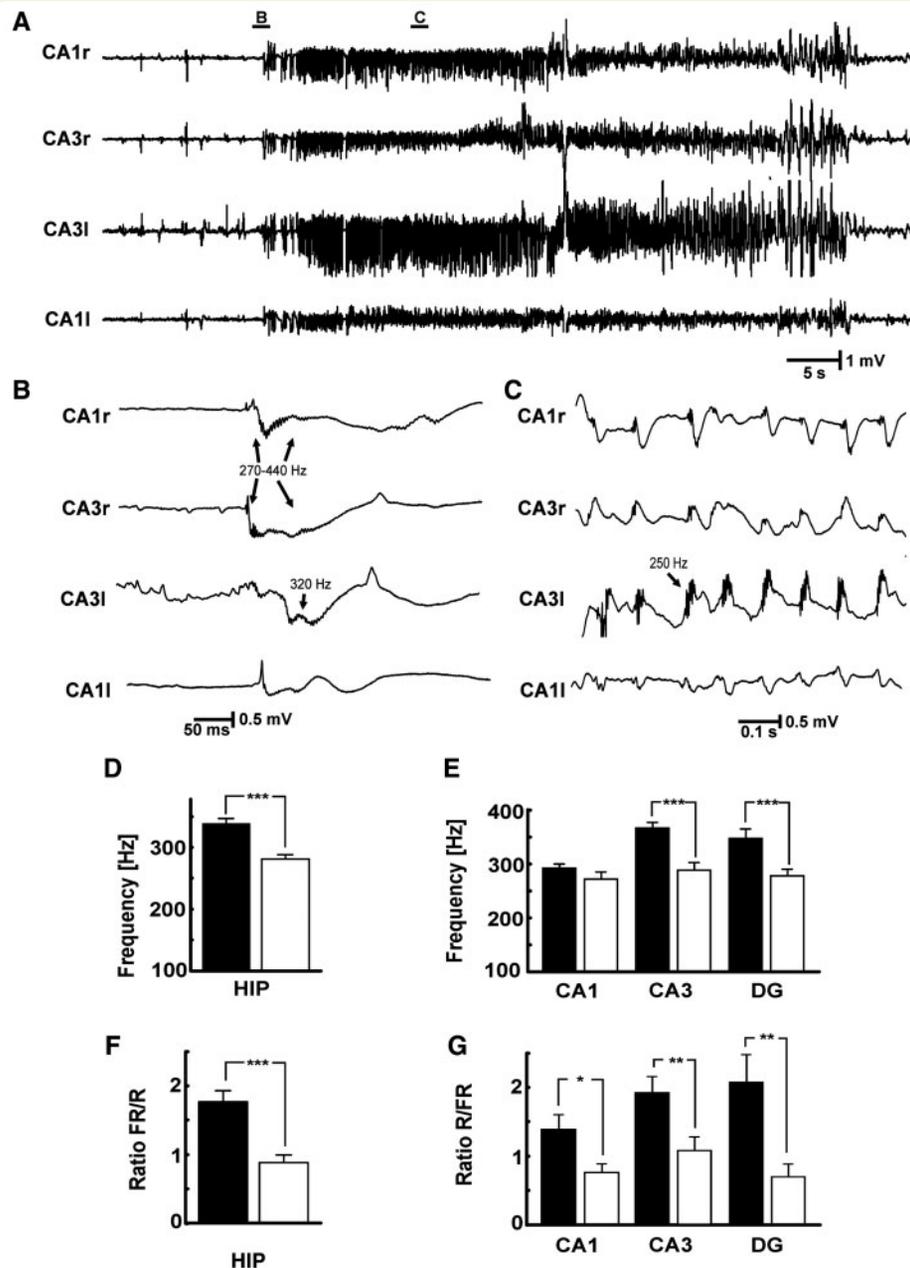
Figure 6 Ictal HFA. (**A**) Typical seizure activity observed in tetanus toxin model of epilepsy: example of a seizure with 'hypersynchronous' onset. (**B**) Seizure onset occurs suddenly and is characterized by bilateral synchronous slow discharges that were first recorded in ipsilateral CA3 and propagated to ipsilateral CA1 and to the contralateral hippocampus. The HFA superimposed on this discharge was initially 440 Hz and later decreased to 270 Hz. HFA was also present in contralateral CA1. (**C**) HFA observed during ictal discharges. (**D**) Comparison of first spectral moment of ictal onset HFA between ipsi- and contralateral hippocampus. (**E**) Regional values of the first spectral moments. (**F**) Fast ripple (FR)/ripple (R) power ratio at ictal onset in the two hippocampi. (**G**) Regional differences of the ratios of fast ripples/ripples. Significance values are *$P < 0.05$, **$P < 0.01$, ***$P < 0.001$. Only raw data are shown.

Perhaps the most specific theory for fast ripples proposes they emerge from ripple activity (Foffani et al., 2007), when ephaptic coupling is weakened by neuronal loss and/or when spike firing reliability is reduced by increased synaptic noise. The theory derives from fast ripples found in vitro in CA3 of hippocampal slices from pilocarpine-treated animals (Foffani et al., 2007), and from the previous in vivo association of fast ripples with substantial

neuronal loss in animal models and human recordings (Bragin et al., 1999b; Staba et al., 2007). Foffani et al. (2007) correlated fast ripples with the severity of cell loss, and attributed the relationship to a decreased efficiency of ephaptic coupling between the more widely spaced neurons. This would result in the population of synchronously firing pyramidal cells that would otherwise generate ripple activity splitting into smaller neuronal assemblies

Figure 7 Histology from hippocampus exhibiting interictal discharges with HFA. (**A**) Interictal discharge recorded in the ipsilateral CA3 with superimposed HFA progressing from 333 to 187 Hz. (**B**) Interictal discharge from the ipsilateral dentate gyrus (DG) with superimposed HFA at 362 Hz. (**C**) Histology of ipsilateral hippocampus showing electrode track (Nissl stain). (**D**) Detail of dentate gyrus histology. (**E**) Detail of CA3 histology. (**F**) Detail of CA1 histology. In **A** and **B**, top trace is raw data and the bottom is band-pass filtered 100–600 Hz. Note absence of hippocampal sclerosis and substantial neuronal loss. s.g. = stratum granulosum; s.p. = stratum pyramidale; s.o. = stratum oriens; s.r. = stratum radiatum. See also Jefferys et al. (1992).

each generating independent ripple activity, which collectively result in higher-frequency, lower-amplitude ripples. The tetanus toxin model of temporal lobe epilepsy, as implemented here, is non-lesional: most animals lack hippocampal sclerosis and detectable neuronal loss; a minority, fewer than 10%, of animals do have a focal loss of CA1 pyramidal cells reminiscent of hippocampal sclerosis, extending 1–2 mm (Jefferys et al., 1992). Injecting similar, comfortably sub-lethal, doses of 10–20 mouse LD_{50} into the ventral hippocampus results in similar focal lesions of CA1 in between 0 and 30% of cases (Hawkins and Mellanby, 1987; Shaw et al., 1990, 1994; Mitchell et al., 1995, 1996; Mellanby et al., 1997). There is some evidence that ventral injections can result in a higher incidence of lesions than dorsal (Shaw et al., 1990), and can lead to a loss of about one-third of hilar somatostatin neurons

by 8 weeks after injection, but not at 4 weeks (Mitchell et al., 1995). Very high doses of tetanus toxin, e.g. 1000 mouse minimum lethal doses, produce substantial neuronal loss and mortality within 7–10 days (Bagetta et al., 1990) (the dose-response curve for tetanus toxin is steep so that for a given batch LD_{50} is a little higher, by perhaps 2- to 4-fold, than the minimum lethal dose). The neuronal loss and mortality in these studies proved to be dose-dependent, being absent with 500 minimum lethal doses and mortality being higher and earlier with 2000 minimum lethal doses (Bagetta et al., 1990). The rats investigated in the present study were routinely processed for histological verification of electrode and injection sites, and none had discernable neuronal loss. The presence of prominent fast ripples in the absence of cell loss in the tetanus toxin model shows that neuronal loss is not prerequisite for fast ripples.

Reduced spike-timing reliability has also been implicated in the generation of fast ripples (Foffani et al., 2007). Essentially the latency to synaptically evoked action potentials becomes less predictable in epileptic tissue. This has been attributed to abnormally intense spontaneous synaptic activity superimposed on the experimental afferent stimulation; the additional synaptic activity was thought to be a consequence of sprouting of excitatory axon collaterals (Foffani et al., 2007). There are important differences between the fast ripples reported by Foffani et al. (2007) and the present results: the former appear to be a harmonic of the underlying ripple activity while the latter can occur in the absence of ripples. However, synaptic noise could be a factor in the tetanus toxin model given the sprouting that has been reported structurally for mossy fibres in dentate gyrus (Mitchell et al., 1996) and functionally for CA1 pyramidal cells (Vreugdenhil et al., 2002).

Epileptic high-frequency activity can be observed bilaterally; the contralateral hippocampus generally has slower frequencies than the injected, but in some cases is capable of generating fast ripple frequencies. Previous observations showed substantial involvement of the contralateral hippocampus in the epileptic syndrome evoked by unilateral hippocampal injection (Jefferys and Empson, 1990; Finnerty and Jefferys, 2002) and slices from the contralateral hippocampus maintained the ability to generate interictal discharges more frequently than injected hippocampus (Jefferys, 1989). Differences in HFA distribution and its properties are in accordance with the previous observation that ipsilateral and contralateral hippocampus possess different underlying epileptogenic mechanisms (Empson and Jefferys, 1993; Whittington and Jefferys, 1994) characterized by distinct impairments of inhibition. The primary focus was characterized by transient (1–2 week) abolition of fast and slow inhibitory postsynaptic potentials. In the secondary focus, fast and slow inhibition was preserved but required stronger interneuronal stimulation to be evoked, suggesting lower intrinsic interneuronal excitability. If synchronization of principal neuronal firing depended on interneuronal firing then the absence of inhibition could explain the hyperexcitability and less precise co-firing of pyramidal cells in primary focus, and shift towards higher frequencies. The loss of inhibitory postsynaptic potentials in primary focus during the first 2–3 weeks after injection argues against the hypothesis that HFA is summated inhibitory postsynaptic potentials on pyramidal cells (Ylinen et al., 1995).

The present study shows that neuronal loss is not necessary for the fast ripples that have previously been associated with epileptic foci. Their selective appearance in the injected hippocampus provides a potential marker for the epileptic tissue under conditions where the slower components of epileptic discharges (mainly interictal), can appear bilaterally synchronous. Fast ripples are a candidate marker for epileptic foci under wider conditions than tissue with extensive neuronal loss.

At present, treatment of patients with non-lesional epilepsy represents a challenge and the future direction of modern epilepsy surgery. The main limitation in these patients is the uncertainty of the localization of the epileptogenic and seizure onset zones. Improving presurgical workup to localize the precise epileptogenic zone in these patients requires novel approaches and better knowledge about the underlying pathophysiological mechanisms. The work presented here suggests that detection of fast ripples could help to improve identification and localization of epileptogenic zones in patients with non-lesional epilepsy.

Acknowledgements

Funding

Supplementary material

Supplementary material is available at *Brain* online.

References

Allen PJ, Fish DR, Smith SJ. Very high-frequency rhythmic activity during SEEG suppression in frontal lobe epilepsy. Electroencephalogr Clin Neurophysiol 1992; 82: 155–9.

Axmacher N, Mormann F, Fernandez G, Elger CE, Fell J. Memory formation by neuronal synchronization. Brain Res Rev 2006; 52: 170–82.

Bagetta G, Nistico G, Bowery NG. Prevention by the NMDA receptor antagonist, MK801 of neuronal loss produced by tetanus toxin in the rat hippocampus. Br J Pharmacol 1990; 101: 776–80.

Bikson M, Fox JE, Jefferys JGR. Neuronal aggregate formation underlies spatiotemporal dynamics of nonsynaptic seizure initiation. J Neurophysiol 2003; 89: 2330–3.

Bragin A, Azizyan A, Almajano J, Wilson CL, Engel J Jr. Analysis of chronic seizure onsets after intrahippocampal kainic acid injection in freely moving rats. Epilepsia 2005; 46: 1592–8.

Bragin A, Engel J Jr, Wilson CL, Fried I, Mathern GW. Hippocampal and entorhinal cortex high-frequency oscillations (100–500 Hz) in human epileptic brain and in kainic acid-treated rats with chronic seizures. Epilepsia 1999a; 40: 127–37.

Bragin A, Engel J Jr, Wilson CL, Vizentin E, Mathern GW. Electrophysiologic analysis of a chronic seizure model after unilateral hippocampal KA injection. Epilepsia 1999b; 40: 1210–21.

Bragin A, Wilson CL, Almajano J, Mody I, Engel J Jr. High-frequency oscillations after status epilepticus: epileptogenesis and seizure genesis. Epilepsia 2004; 45: 1017–23.

Bragin A, Wilson CL, Engel J Jr. Chronic epileptogenesis requires development of a network of pathologically interconnected neuron clusters: a hypothesis. Epilepsia 2000; 41(Suppl 6): S144–52.

Draguhn A, Traub RD, Schmitz D, Jefferys JGR. Electrical coupling underlies high-frequency oscillations in the hippocampus in vitro. Nature 1998; 394: 189–92.

Dzhala VI, Staley KJ. Mechanisms of fast ripples in the hippocampus. J Neurosci 2004; 24: 8896–906.

Dudek FE, Snow RW, Taylor CP. Role of electrical interactions in synchronization of epileptiform bursts. Adv Neurol 1986; 44: 593–617.

Empson RM, Jefferys JGR. Synaptic inhibition in primary and secondary chronic epileptic foci induced by intrahippocampal tetanus toxin in the rat. J Physiol 1993; 465: 595–614.

Finnerty GT, Jefferys JGR. Functional connectivity from CA3 to the ipsilateral and contralateral CA1 in the rat dorsal hippocampus. Neuroscience 1993; 56: 101–108.

Finnerty GT, Jefferys JGR. Investigation of the neuronal aggregate generating seizures in the rat tetanus toxin model of epilepsy. J Neurophysiol 2002; 88: 2919–27.

Fisher RS, Webber WR, Lesser RP, Arroyo S, Uematsu S. High-frequency EEG activity at the start of seizures. J Clin Neurophysiol 1992; 9: 441–48.

Foffani G, Uzcategui YG, Gal B, Menendez de la Prida L. Reduced spike-timing reliability correlates with the emergence of fast ripples in the rat epileptic hippocampus. Neuron 2007; 55: 930–41.

Grenier F, Timofeev I, Steriade M. Neocortical very fast oscillations (ripples, 80-200 Hz) during seizures: intracellular correlates. J Neurophysiol 2003; 89: 841–52.

Hawkins CA, Mellanby JH. Limbic epilepsy induced by tetanus toxin - a longitudinal electroencephalographic study. Epilepsia 1987; 28: 431–44.

Jacobs J, Levan P, Chander R, Hall J, Dubeau F, Gotman J. Interictal high-frequency oscillations (80-500 Hz) are an indicator of seizure onset areas independent of spikes in the human epileptic brain. Epilepsia 2008; 49: 1893–907.

Jefferys JGR. Chronic epileptic foci in vitro in hippocampal slices from rats with the tetanus toxin epileptic syndrome. J Neurophysiol 1989; 62: 458–68.

Jefferys JGR, Empson RM. Development of chronic secondary epileptic foci following intrahippocampal injection of tetanus toxin in the rat. Exp Physiol 1990; 75: 733–6.

Jefferys JGR, Evans BJ, Hughes SA, Williams SF. Neuropathology of the chronic epileptic syndrome induced by intrahippocampal tetanus toxin in rat: preservation of pyramidal cells and incidence of dark cells. Neuropathol Appl Neurobiol 1992; 18: 53–70.

Jefferys JGR. Nonsynaptic modulation of neuronal activity in the brain: electric currents and extracellular ions. Physiol Rev 1995; 75: 689–723.

Jefferys JGR, Walker MC. Tetanus toxin model of focal epilepsy. In: Pitkanen A, Schwartzkroin PA, Moshe SL, editors. Models of seizures and epilepsy. Amsterdam: Elsevier Academic Press; 2005. p. 407–14.

Jiruska P, Csicsvari J, Powell AD, Fox JE, Chang WC, Vreugdenhil M, et al. High-frequency network activity, global increase in neuronal activity and synchrony expansion precede epileptic seizures in vitro. J Neurosci 2010 (In Press).

Li X, Yao X, Fox J, Jefferys JGR. Interaction dynamics of neuronal oscillations analysed using wavelet transforms. J Neurosci Methods 2007; 160: 178–85.

Mellanby J, George G, Robinson A, Thompson P. Epileptiform syndrome in rats produced by injecting tetanus toxin into the hippocampus. J Neurol Neurosurg Psychiat 1997; 40: 404–14.

Mitchell J, Gatherer M, Sundstrom LE. Loss of hilar somatostatin neurons following tetanus toxin- induced seizures. Acta Neuropathol (Berl) 1995; 89: 425–30.

Mitchell J, Gatherer M, Sundstrom LE. Aberrant Timm-stained fibres in the dentate gyrus following tetanus toxin-induced seizures in the rat. Neuropathol Appl Neurobiol 1996; 22: 129–35.

Mitra PP, Pesaran B. Analysis of dynamic brain imaging data. Biophys J 1999; 76: 691–708.

Shaw JAG, Perry VH, Mellanby J. Tetanus toxin-induced seizures cause microglial activation in rat hippocampus. Neurosci Lett 1990; 120: 66–9.

Shaw JAG, Perry VH, Mellanby J. MHC class II expression by microglia in tetanus toxin-induced experimental epilepsy in the rat. Neuropathol Appl Neurobiol 1994; 20: 392–8.

Snow RW, Dudek FE. Synchronous epileptiform bursts without chemical transmission in CA2, CA3 and dentate areas of the hippocampus. Brain Res 1984; 298: 382–5.

Staba RJ, Frighetto L, Behnke EJ, Mathern GW, Fields T, Bragin A, et al. Increased fast ripple to ripple ratios correlate with reduced hippocampal volumes and neuron loss in temporal lobe epilepsy patients. Epilepsia 2007; 48: 2130–8.

Staba RJ, Wilson CL, Bragin A, Fried I, Engel J Jr. Quantitative analysis of high-frequency oscillations (80-500 Hz) recorded in human epileptic hippocampus and entorhinal cortex. J Neurophysiol 2002; 88: 1743–52.

Vreugdenhil M, Hack SP, Draguhn A, Jefferys JGR. Tetanus toxin induces long-term changes in excitation and inhibition in the rat hippocampal CA1 area. Neuroscience 2002; 114: 983–94.

Whittington MA, Jefferys JGR. Epileptic activity outlasts disinhibition after intrahippocampal tetanus toxin in the rat. J Physiol 1994; 481: 593–604.

Worrell GA, Parish L, Cranstoun SD, Jonas R, Baltuch G, Litt B. High-frequency oscillations and seizure generation in neocortical epilepsy. Brain 2004; 127: 1496–506.

Ylinen A, Bragin A, Nadasdy Z, Jando G, Szabo I, Sik A, et al. Sharp wave-associated high-frequency oscillation (200 Hz) in the intact hippocampus: network and intracellular mechanisms. J Neurosci 1995; 15: 30–46.